Optics Communications 445 (2019) 296–300

Contents lists available at ScienceDirect

Optics Communications

journal homepage: www.elsevier.com/locate/optcom

Narrow linewidth DBR laser based on high order Bragg grating defined by i-line lithography

Hong Chen [a,b], Peng Jia [a,*], Chao Chen [a,*], Li Qin [a], Yongyi Chen [a], Youwen Huang [a], Yongqiang Ning [a], Lijun Wang [a]

[a] State Key Laboratory of Luminescence and Applications, Changchun Institute of Optics, Fine Mechanics and Physics, Chinese Academy of Sciences, Changchun 130033, China

[b] University of Chinese Academy of Sciences, Beijing 100049, China

ARTICLE INFO

Keywords:
Semiconductor laser
Distributed Bragg reflector laser
High-order grating
Narrow linewidth spectrum

ABSTRACT

In order to obtain narrow linewidth semiconductor laser around 1564 nm, we design a distributed Bragg reflector (DBR) laser with high-order Bragg gratings (HOBGs) using butterfly encapsulation. The DBR laser is fabricated only by i-line lithography technology with grating period of 4. 84 μm, groove width of 1. 5 μm and grating length of 72 μm on a strip width of 4 μm. The 1mm-long devices achieved an output power of 9.9 mW and a side mode suppression ratio (SMSR) more than 30 dB without facet coating at an injection current of 80 mA. The lasers showed ultra-narrow Lorentz linewidth of 70 kHz. This paper provides a simple method for large-scale production of narrow linewidth semiconductor lasers.

1. Introduction

Lasers operating in the wavelength region of 1.5-2 μm have a high water absorption coefficient, which has high threshold power of eye damage, and therefore it has an eye-safe characteristic [1–3]. What is more, it has the advantages of small sizes, high power, narrow spectral linewidth, and easy preparation. These advantages make narrow linewidth semiconductor lasers around 15xx nm essential in many important applications such as wavelength division multiplexing, coherent communication, and laser radar [4–7].

In recent years, narrow linewidth semiconductor lasers around 15xx nm have drawn considerable attention. The Tampere University of Technology and the University of Ottawa reported the laterally-coupled distributed feedback (DFB) laser achieving ultra-narrow linewidth laser with an output power greater than 6 mW, SMSR greater than 50 dB and single mode spectral Lorentz linewidth less than 200 kHz [8,9]. By introducing several slot structures to the waveguide of a Fabry Perot (FP) laser, Wang Yin of Zhejiang University produced a slot-Fabry Perot (SFP) laser with a linewidth of only 80 kHz and an output power of 8 mW [10]. H. Yang et al. of the Tyndall National Research Institute, reported a multimode interference waveguide (MMI) laser based on teardrop structure, which achieved a narrow linewidth laser output with a Lorentz linewidth of 75 kHz and an SMSR greater than 30 dB [11]. The University of Trinity also reported a narrow linewidth laser using a regional slot structure [12]. The narrow linewidth semiconductor lasers reported above mostly relied on complex and expensive high precision lithography and secondary epitaxial technology which largely limit the large scale production applications of narrow linewidth semiconductor lasers.

To solve these problems in this paper, a narrow linewidth high-order grating DBR laser only using i-line lithography is designed by analyzing the selection characteristics of HOBGs for DBR laser cavity modes. Under injection current of 80 mA, the output power from each facet is 9.9 mW, and the linewidth is only 70 kHz. A narrow linewidth laser output with a SMSR more than 30 dB is achieved. It provides a simple method which avoids the high cost and low yield problem brought by the complicated and expensive electron beam lithography technology and the secondary epitaxial technology for large-scale production of narrow linewidth semiconductor lasers.

2. Laser structure and fabrication

2.1. The structure of devices

The schematic diagram of our device is shown in Fig. 1(a). The vertical structure grown on n-InP substrate consists of a n-InP cladding, n-AlGaInAs optical confinement layer, multi-quantum well active layers, p-AlGaInAs optical confinement layer, p-InP cladding and p-GaInAs cap layer. The Inp/GaInAsP multi-quantum well (MQW) structure has been grown by metal–organic chemical vapor deposition (MOCVD). Fig. 1(b) shows several periodicities of the gratings under scanning electron microscopy.

* Corresponding authors.
E-mail addresses: jiapeng@ciomp.ac.cn (P. Jia), chenc@ciomp.ac.cn (C. Chen).

https://doi.org/10.1016/j.optcom.2019.03.062
Received 2 February 2019; Received in revised form 8 March 2019; Accepted 24 March 2019
Available online 20 April 2019

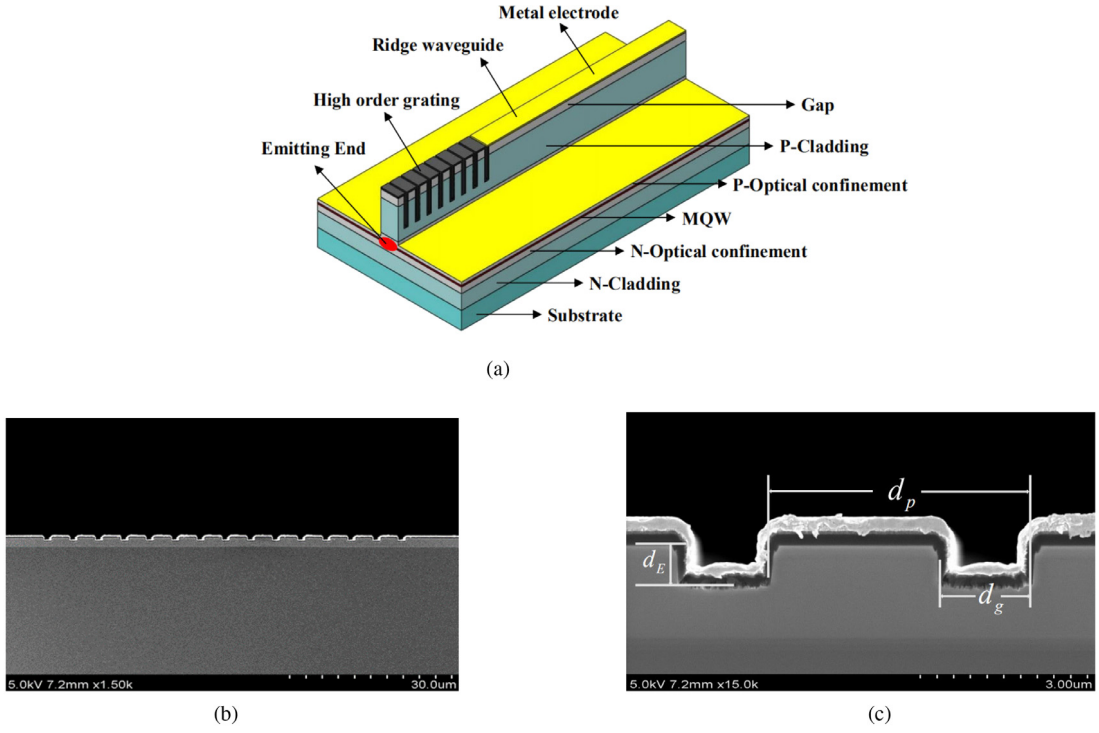

Fig. 1. (a) Structure diagram of HOBGs DBR laser (b) scanning electron microscope (SEM) picture of HOBGs (c) SEM image of the enlarged grating portion.

2.2. The design of device

In order to obtain narrow linewidth emission, we design the grating parameters using the commercial software COMSOL Multiphysics. In the following equation, d_p represents the period of gratings, d_g is the width of grooves and d_E is the etch depth of gratings [13]:

$$d_p = \frac{m\lambda}{4n_{eff,ave}}, m = 2, 4, 6 \cdots \cdots \quad (1)$$

$$d_g = \frac{m_g\lambda}{4n_{eff,g}}, m_g = 1, 3, 5 \cdots \cdots \quad (2)$$

where m and m_g are integers, λ is the mode gain peak, $n_{eff,g}$ and $n_{eff,ave}$ are the effective refractive index of the material in the groove and the average effective refractive index of the laser waveguide, respectively.

The effective refractive index of the laser material is calculated to be 3.163417 by solving partial differential equations using COMSOL Multiphysics. The HOBGs introduce perturbation into the effective refractive index of the waveguide, and regulate the loss of the optical mode in the resonant cavity so that the specific mode is strengthened to greatly reduce the linewidth. We prepared HOBGs by i-line lithography with a pattern resolution of about 1 μm. In the case of a duty cycle of 69%, the groove width should not be less than 1 μm. According to Eqs. (1) and (2), we designed the HOBGs with a period dp of 4.84 μm and a groove width dg of 1.5 μm using the transfer matrix method. The reflectance spectrum at different etch depths is obtained as shown in Fig. 2. When the m_g is odd, the length of the HOBGs is an odd multiple a quarter of the wavelength, and the highest reflectivity can be achieved [14], thereby improving the feedback effect of the HOBGs on the cavity. For Bragg gratings, the longer the gratings, the greater the photon lifetime and the narrower the linewidth. But the length of gratings cannot be too long, because it will increase quantum noise and loss. So we must reasonably design the length of the gratings. Therefore, we design the length of the HOBGs to be 72 μm. The effective refractive index of the optical mode in HOBGs is closely related to the etching depth of the grating. The deeper the grating is etched, the higher feedback in the cavity will be received. The smaller the effective refractive index of the optical mode in HOBGs is, the larger index contrast between the HOBGs and the waveguide will be, and higher loss can be achieved to make it easier to obtain narrow linewidth device. However, the grating trench cannot be over-etched, otherwise it will lead to high order scattering enhancement, which will increase the power loss of the waveguide. The etching depth d_E of the grating trench is designed to be 1.2 μm, providing a narrow linewidth output while providing sufficient feedback. We calculated the reflectance and loss at different etch depths. The variation of the etching depths only affect the reflection efficiency (from 7% at 1.0 μm to 16% at 1.3 μm), not the central wavelength. Only the wavelength with higher reflection (lower mirror loss and scattering loss) can lase. Combined with the reflection and loss spectra, the etch depth of the device allows for a range of tolerances. Applying the above data to calculate the scattering loss, transmission spectra at different etch depths are shown in Figs. 2(b) and 2(c) below:

In Fig. 2(a), we can see that the high-order grating structure provides a strong reflection spectrum at $\lambda \approx 1562$ nm. In Figs. 2(b) and 2(c) we can see the transmission and loss are minimum around 1562 nm, it indicates that the grating structure can enhance the feedback strength of the mode at $\lambda \approx 1562$ nm, suppressing other side modes in mode competition, and achieving narrow linewidth laser lasing around 1562 nm.

The spectral linewidth characterization method of semiconductor laser is mainly self-heterodyne method and power spectral density (PSD) measurement method [15–17]. The power spectral density can reflect the spectral characteristics of the lasers frequency noise in a very detailed way, and the included frequency noise information is much larger than the linewidth. Therefore, the power spectral density method is used to characterize the spectral linewidth of the laser in this paper.

The linewidth of semiconductor lasers is mostly caused by white noise [18,19]. So this paper only considers the effect of white noise on linewidth.

When there is only white noise in the frequency noise of the laser, the line type of the output spectrum is a Lorentz line type, the value of the linewidth is also gradually approaching the fixed value and no longer changes. The relationship between linewidth and frequency

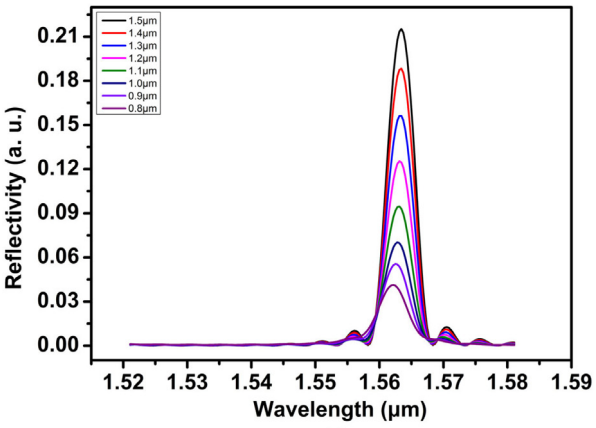

(a)

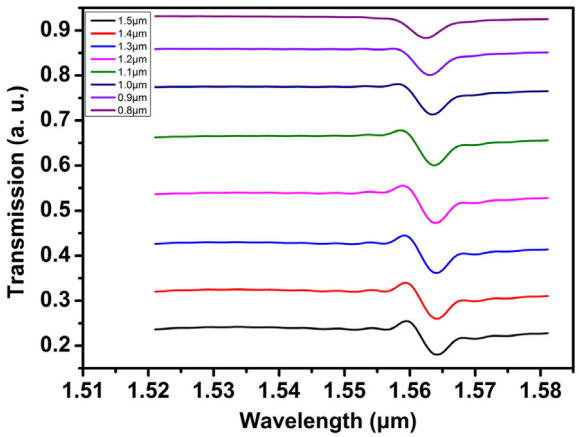

(b)

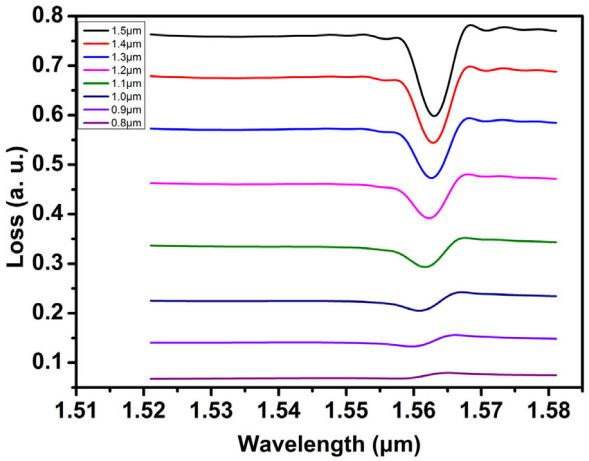

(c)

Fig. 2. (a) Reflection spectrum (b) transmission loss (c) loss spectrum of HOBGs DBR laser at different etch depths.

spectral density of white noise is [20]:

$$\triangle f = \pi S_0 \tag{3}$$

where $\triangle f$ represents the linewidth, S_0 represents the value of white noise frequency spectral density, the unit is Hz^2/Hz. The linewidth is only related to the frequency noise spectral density.

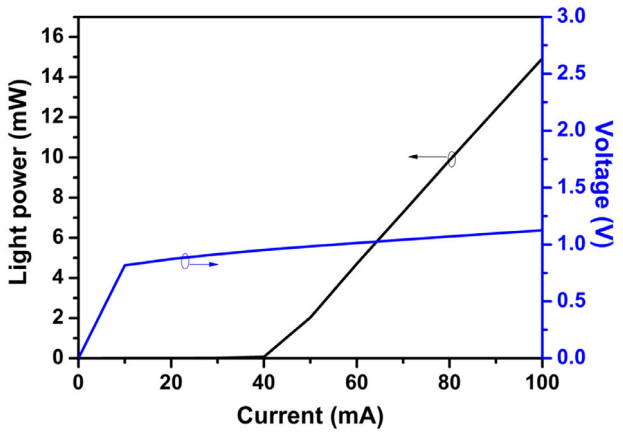

Fig. 3. The light power–current–voltage curve graph of HOBGs laser.

2.3. The fabrication of devices

The narrow linewidth DBR semiconductor laser integrates a set of high order grating structures with a period of 4.84 μm on the waveguide of the ridge FP laser to realize a single longitudinal mode narrow linewidth laser output, where the length of the grating region is about 72 μm. First the HOBGs with a period of 4.84 μm were defined by i-line lithography on the wafer. Then the grooves of the gratings with a width of 1.5 μm were etched into the wafer via inductively coupled plasma etching (ICP). After the implementation of the gratings, trenches were etched on either side of the gratings to create ridge waveguides (RWs) with a ridge width of 4 μm. A silica layer with suitable thickness for passivation was deposited on top of the HOBGs by plasma enhanced chemical vapor deposition (PECVD). P-contact metallization was grown by the magnetron sputtering technology. The thickness of the chip was then reduced and polished for N-contact metallization. Then the chip was cleaved. The butterfly package is used to make the laser chip into a temperature control laser module for performance testing.

3. Results and discussion

In order to achieve accurate measurement of laser spectral linewidth and power characteristics, the devices were mounted p-side up on simple COS-mount heat sinks, and then the COS module and the Thermo Electric Cooler (TEC) heat sink are integrated into the butterfly shell with connecting to a TEC temperature control device to maintain stationary temperature (25 °C) for testing.

The power–voltage–current characteristics for 1 mm cavity length device without facet coating in CW operation are shown in Fig. 3. Fig. 3 shows that the threshold current is 40 mA. And the slope efficiency is up to 0.25 W/A, which is larger than 0.21 W/A of the previously reported narrow linewidth slotted Fabry Perot laser using deep etched trenches [10]. The voltage curve is kink-free, but the power curve shows a small kink near 50 mA. We measured the wavelength change at a smaller current increment (0.5 mA) and found no typical mode hopping phenomenon. We think it may be due to a lift-up of the degeneracy of the single longitudinal lasing mode. High order scattering loss is inevitable due to HOBGs structure, while achieving the single longitudinal mode operation of the device, the threshold value of the laser is increased, the output power is reduced, and the slope efficiency is lowered.

CW spectrum characteristics were measured by the Yokogawa AQ6370C spectrum analyzer and a single-mode fiber with a core diameter of 8 μm and a resolution of 0.02 nm (see Fig. 4). A stable single longitudinal mode spectrum recorded at a current of 80 mA and shown in Fig. 4(a) reveals the linewidth of 70 kHz and SMSR more than 30 dB. In the future research, we can optimize the design of the

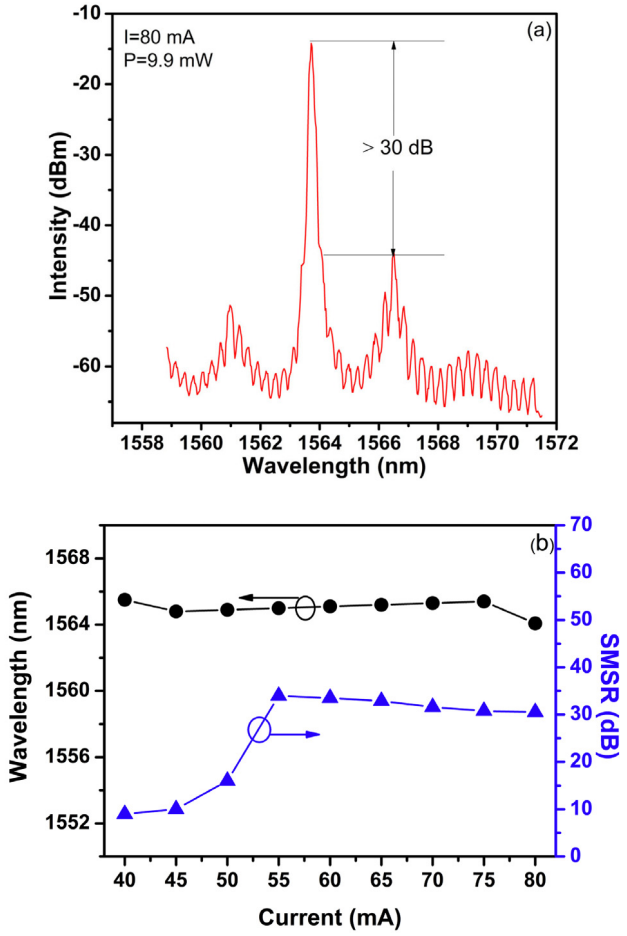

Fig. 4. (a) Spectrum of HOBGs laser at injection current of 80 mA (b) Curve graph of laser wavelength and SMSRs with increasing injection current from 40 mA to 80 mA . (For interpretation of the references to color in this figure legend, the reader is referred to the web version of this article.)

grating parameters, increase the coupling of the grating region, reduce the energy loss, and thus reduce the threshold current to increase the SMSR. We can further optimize the design of etching depth of the grating to increase the mirror loss difference and then increase the SMSR. Also, better AR film coating at the emitting end will help reduce the unwanted FP modes and increase SMSR. Mainly based on the following formula [21]:

$$SMSR(dB) \approx 10\lg\left[\frac{\Delta\alpha + \Delta g}{\delta_G} + 1\right] \tag{4}$$

$$\delta_G = 10^{-3} I_{th}/(I - I_{th})\ \mathrm{cm}^{-1} \tag{5}$$

where $\Delta\alpha$ is the difference of mirror loss (the difference between the mirror loss of the main mode and the mirror loss of the side mode), Δg is the difference of mode gain, I_{th} is the threshold current.

In Fig. 4(b), we see that the injection current increases from 40 mA to 80 mA. The laser wavelength appears to be red-shifted as a whole. But there are two blue shifts at 45 mA and 80 mA. Because the 45 mA injection current just passed the threshold current, the threshold gain difference between the main mode and the side modes is small, and it is impossible to effectively suppress the side modes, so the mode hopping phenomenon occurs. When the current of 80 mA, the self-heating effect of the current injection region is enhanced, and the temperature inside the device rises, especially the temperature of the active region increases, the band gap becomes narrower, and the refractive index increases greatly. Resulting that the gain curve is red-shifted as a whole and the grating structure is an electroless injection region.

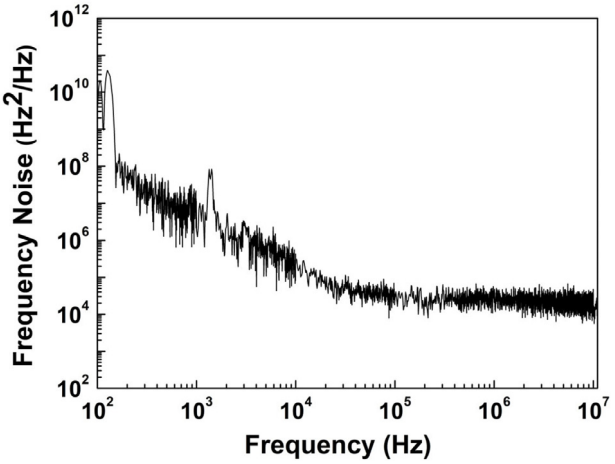

Fig. 5. White noise distribution characteristics of laser.

The refractive index of the material changes slightly with current, and the reflection spectrum changes little, causing the reflectivity of the short-wavelength side mode to increase and a secondary blue shift phenomenon. As the current increases, the SMSR tends to increase first and then decrease. This is because the mode competition is sufficient when the current is increased from 40 mA to 50 mA, the side modes are suppressed, the main mode is gradually enhanced, and the SMSR is increased. When the current is increased from 60 mA to 80 mA, heat accumulation occurs inside the device, causing misalignment of the Bragg wavelength and the gain spectrum, resulting in a weakening of the side modes suppression effect and a decrease in the side mode suppression ratio.

To characterize the spectral linewidth of the laser, the frequency noise of the laser was measured by OE4000 cross-correlation homodyne phase/frequency noise automatic test system of OEwaves Company. And based on the formula (3), the spectral linewidth of the narrow linewidth laser is obtained, as shown in Fig. 5, the device achieved a linewidth of 70 kHz at an injection current of 80 mA and the SMSR of above 30 dB.

4. Conclusions

By using the coupled mode theory to analyze the reflection characteristics of HOBGs, a narrow linewidth distributed reflection (DBR) semiconductor laser based on HOBGs structure is developed, which realizes wavelength peak of 1564 nm and output power of 9.9 mW with the current of 80 mA, the SMSR more than 30 dB, a linewidth of 70 kHz. The preparation of such a HOBGs DBR laser device only requires the use of ordinary ultraviolet lithography technology, which avoids the high cost and low yield problem brought by the complicated and expensive electron beam lithography technology and the secondary epitaxial technology. It provides a simple method for large-scale production of narrow linewidth semiconductor lasers.

Acknowledgments

This work was supported by National Key R&D Program of China (2016YFE0126800); The National Key R&D Program of China (2017YFB0405100); National Natural Science Foundation of China (61874119); Science and Technology Development Project of Jilin Province (20180201014GX).

References

[1] T. Tamanuki, T. Sasaki, M. Kitamura, High power and narrow lateral far-field divergence 1.5-μm eye-safe pulsed laser diodes with flared waveguide, Opt. Quantum Electron. 28 (5) (1996) 513–517.

[2] S. Kallenbach, et al., High-power high-brightness tapered diode lasers and amplifiers for eye-safe operation, in: Lasers & Electro-optics Society, Leos the Meeting of the IEEE, 2004.

[3] A.R. Nehrir, K.S. Repasky, J.L. Carlsten, Eye-safe diode-laser-based micropulse differential absorption lidar (DIAL) for water vapor profiling in the lower troposphere, J. Atmos. Ocean. Technol. 28 (2011) 131–147.

[4] A. Consoli, M. Krakowski, G. Kochem, High-brightness all semiconductor laser at 1.57 μm for space-borne lidar measurements of atmospheric carbon dioxide: device design and analysis of requirements, in: Conference on Laser Sources and Applications II, 2014, pp. 913516.

[5] Kais Dridi, et al., Narrow linewidth 1560 nm InGaAsP split-contact corrugated ridge waveguide DFB lasers, Opt. Lett. 39 (21) (2014) 6197.

[6] Zhechao Wang, A III-V-on-Si ultra-dense comb laser, Light: Sci. Appl. 6 (5) (2017) e16260.

[7] S.R. Selmic, G.A. Evans, T.M. Chou, Single frequency 1550-nm AlGaInAs-InP tapered high-power laser with a distributed Bragg reflector, IEEE Photonics Technol. Lett. 14 (7) (2002) 890–892.

[8] J. Telkkala, J. Viheriala, A. Aho, J. Telkkala, Narrow linewidth laterally-coupled 1.55μm DFB lasers fabricated using nanoimprint lithography, Electron. Lett. 47 (6) (2011) 400–401.

[9] K. Dridi, A. Benhsaien, J. Zhang, Narrow linewidth two-electrode 1560 nm laterally coupled distributed feedback lasers with third-order surface etched gratings, Opt. Express 22 (16) (2014) 19087–19097.

[10] Y. Wang, Y. Yang, S. Zhang, Narrow linewidth single-mode slotted Fabry–Pérot laser using deep etched trenches, IEEE Photonics Technol. Lett. 24 (14) (2012) 1233–1235.

[11] H. Yang, M. Yang, Y. Zhao, Butterfly packaged ultra-narrow linewidth single frequency teardrop laser diode, IEEE Photonics Technol. Lett. 99 (2017) 1–1.

[12] F. Bello, Q.Y. Lu, A. Abdullaev, Linewidth and noise characterization for a partially-slotted, single mode laser, Quantum Electr. IEEE J. 50 (9) (2014) 755–759.

[13] J. Patchell, J. O'Gorman, Specifying the wavelength and temperature tuning range of a Fabry–Perot laser containing refractive index perturbations, Proc. SPIE - Int. Soc. Opt. Eng. 5825 (2005) 1–13.

[14] J. Fricke, W. John, A. Klehr, Properties and fabrication of high-order bragg gratings for wavelength stabilization of diode lasers, Semicond. Sci. Technol. 27 (27) (2012) 055009.

[15] N.V. Bandel, M. Myara, M. Sellahi, et al., Time-dependent laser linewidth: beat-note digital acquisition and numerical analysis, Opt. Express 24 (24) (2016) 27961–27978.

[16] H. Tsuchida, Laser frequency modulation noise measurement by recirculating delayed self-heterodyne method, Opt. Lett. 36 (5) (2011) 681–683.

[17] Tsuchida, Characterization of White and Flicker frequency modulation noise in narrow-linewidth laser diodes, IEEE Photonics Technol. Lett. 23 (11) (2011) 727–729.

[18] K.J. Vahala, A. Yariv, Semiclassical theory of noise in semiconductor lasers-part II, IEEE J. Quantum Electron. 19 (6) (1983) 1102–1109.

[19] J. Mørk, Bistability and low-frequency fluctuations in semiconductor lasers with optical feedback: a theoretical analysis, IEEE J. Quantum Electron. 24 (2) (1988) 123–133.

[20] S. Schilt, N. Bucalovic, V. Dolgovskiy, Fully stabilized optical frequency comb with sub-radian CEO phase noise from a SESAM-modelocked 1.5-μm solid-state laser, Opt. Express 19 (24) (2011) 24171–24181.

[21] Larry A. Coldren, Diode lasers and photonic integrated circuits, Opt. Eng. 36 (2) (1997) 616.